



Supporting Information

for

Size control of nanoparticles synthesized by pulsed laser ablation in liquids using donut-shaped beams

Abdel Rahman Altakroury, Oleksandr Gatsa, Farbod Riahi, Zongwen Fu,
Miroslava Flimelová, Andrei Samokhvalov, Stephan Barcikowski, Carlos Doñate-Buendía,
Alexander V. Bulgakov and Bilal Gökce

Beilstein J. Nanotechnol. **2025**, *16*, 407–417. doi:10.3762/bjnano.16.31

Additional experimental data

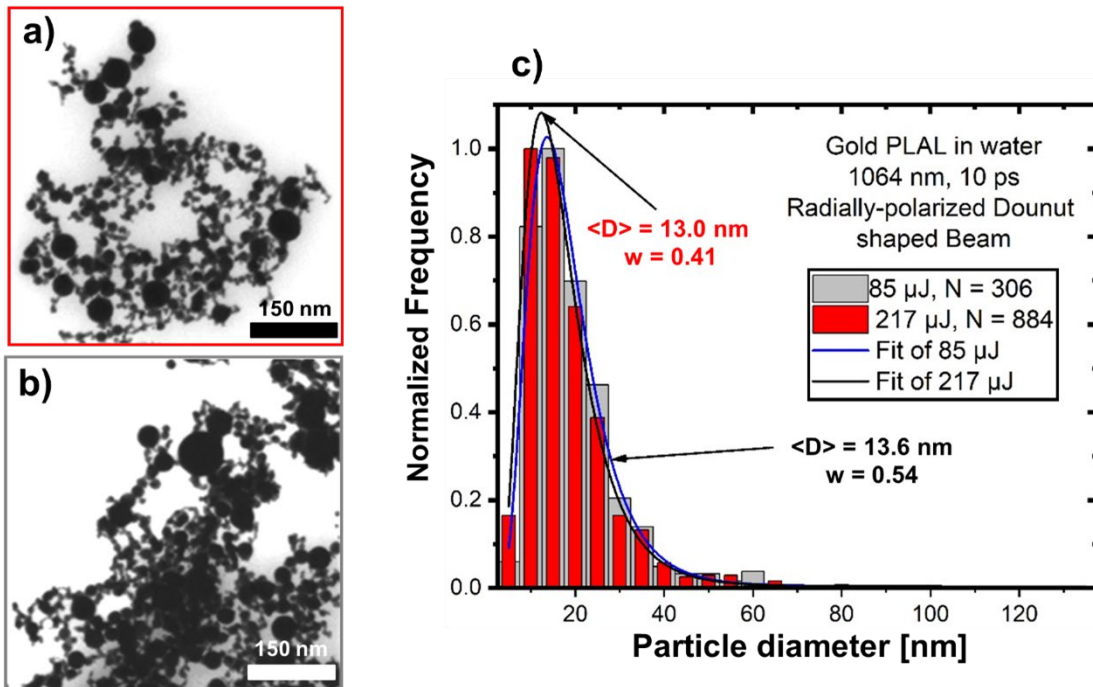


Figure S1: Comparison of gold NPs produced by PLAL with radially polarized donut-shaped laser beams at pulse energies of 85 and 217 μ J. (a, b) SEM micrographs of NPs obtained using pulse energies of 85 and 217 μ J, respectively. (c) NP size distributions showing the number of analyzed NPs (N), the median diameter ($\langle D \rangle$), and the polydispersity index (w) values derived from the log-normal approximations (solid lines).

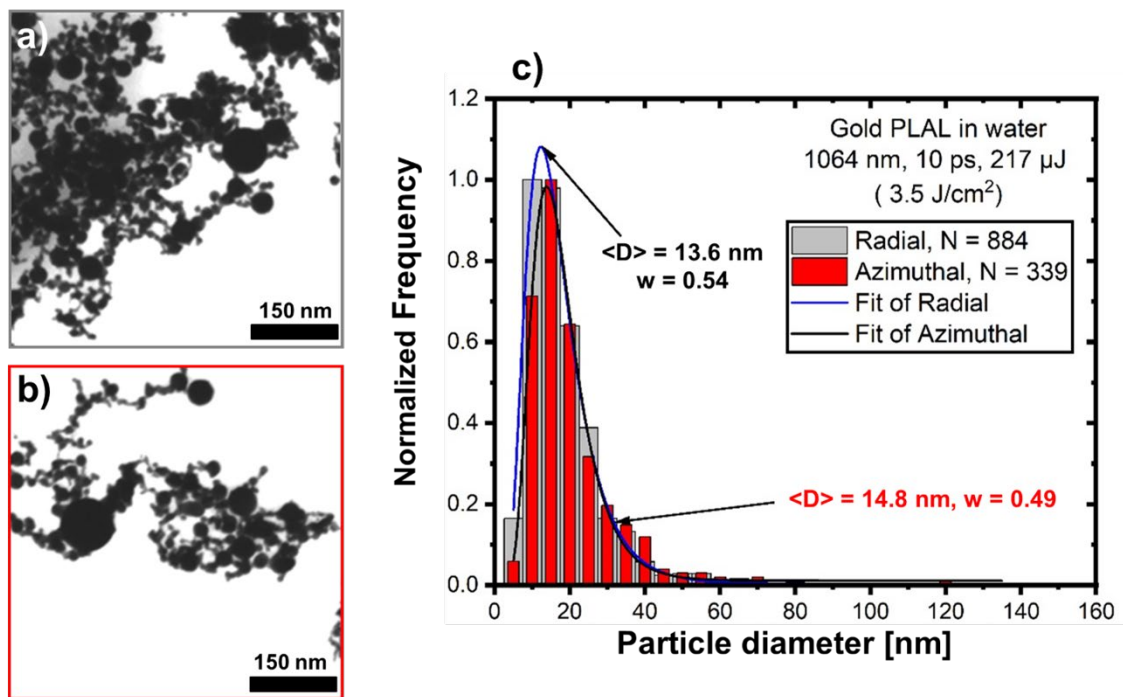


Figure S2: Comparison of gold NPs produced by PLAL with radially polarized donut-shaped and azimuthally polarized donut-shaped laser beams at a pulse energy of 217 μJ . (a, b) SEM micrographs of NPs obtained using the radially polarized donut-shaped and azimuthally polarized donut-shaped beams, respectively. (c) NP size distributions showing the number of analyzed NPs (N), the median diameter ($\langle D \rangle$), and the polydispersity index (w) values derived from the log-normal approximations (solid lines).

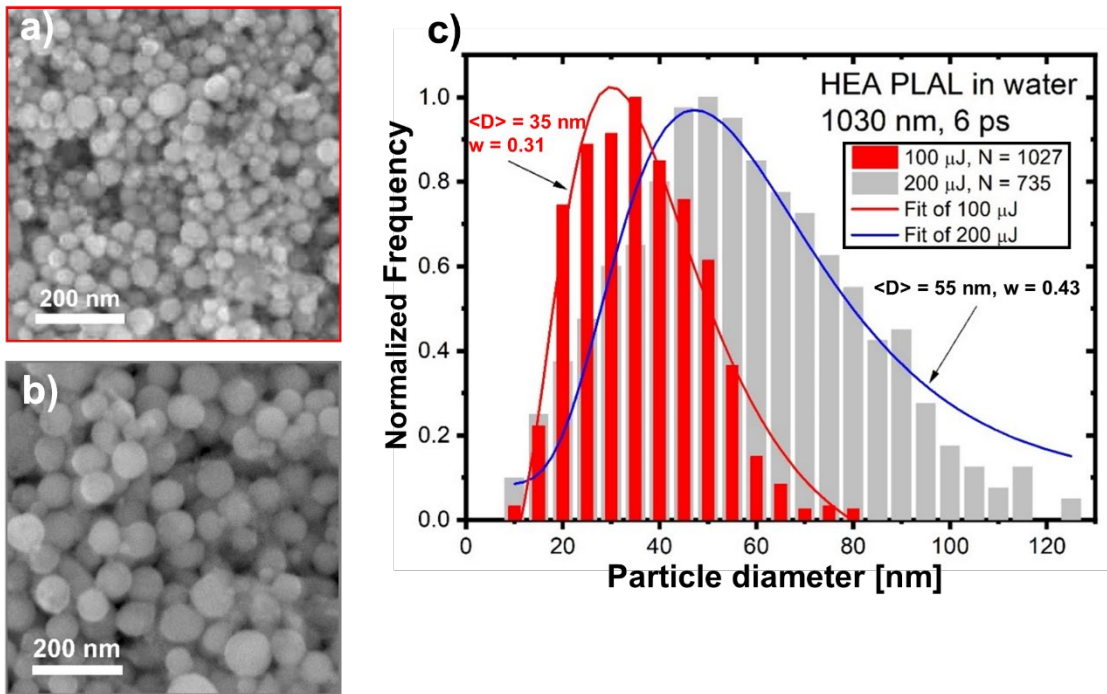


Figure S3: Comparison of HEA NPs produced by PLAL with radially polarized donut-shaped laser beams at pulse energies of 100 and 200 μ J. (a, b) SEM micrographs of NPs obtained using pulse energies of 100 and 200 μ J, respectively. (c) NP size distributions showing the number of analyzed NPs (N), the median diameter ($\langle D \rangle$), and the polydispersity index (w) values derived from the log-normal approximations (solid lines).

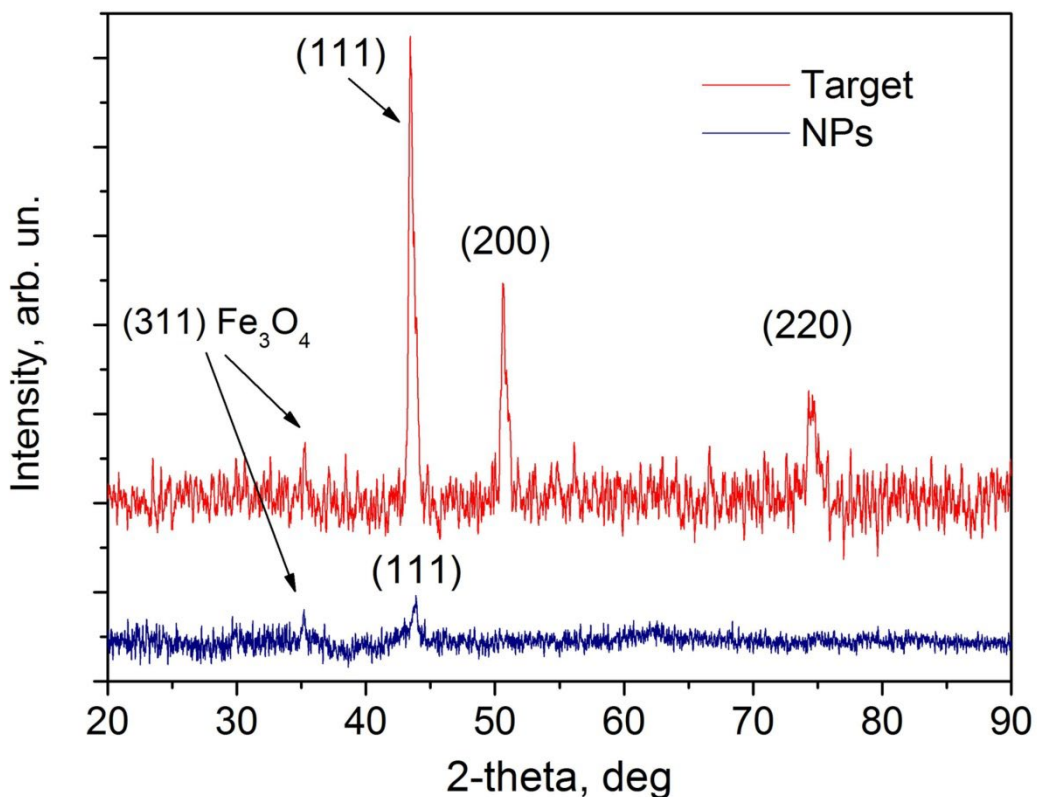


Figure S4: XRD patterns for the HEA target and NPs generated by PLAL by a donut-shaped laser beam at a pulse energy of $100 \mu\text{J}$. The crystalline HEA phase is represented by peaks corresponding to (111), (200), and (220) Bragg reflections of the face-centered cubic lattice. An additional (311) peak at $2\theta = 35.2^\circ$ corresponds to the cubic Fe_3O_4 phase. The height ratio of the oxide peak to the (111) peak is higher for NPs.